Delineation and Analysis of Chromosomal Regions Specifying Yersinia pestis

Anne Derbise, Viviane Chenal-Francisque, Christèle Huon, Corinne Fayolle, Christian Demeure, Béatrice Chane-Woon-Ming, Claudine Médigue, B. Joseph Hinnebusch, Elisabeth Carniel

Delineation and analysis of chromosomal regions specifying *Yersinia pestis*

Anne Derbise[1*], Viviane Chenal-Francisque[1], Christèle Huon[1], Corinne Fayolle[1], Christian E. Demeure [1], Béatrice Chane-Woon-Ming[2], Claudine Médigue[2], B. Joseph Hinnebusch[3] and Elisabeth Carniel[1]

[1]*Yersinia* Research Unit, Institut Pasteur, 28 rue du Dr. Roux, 75724 Paris Cedex 15, France.

[2] Commissariat à l'Energie Atomique (CEA), Direction des Sciences du Vivant, Institut de Génomique, Genoscope & CNRS-UMR 8030, Laboratoire d'Analyse Bioinformatique en Génomique et Métabolisme, 2 rue Gaston Crémieux, 91057 Evry Cedex, Evry cedex F-91006, France.

[3] Laboratory of Zoonotic Pathogens, Rocky Mountain Laboratories, National Institute of Allergy and Infectious Diseases, National Institutes of Health, Hamilton, MT 59840, USA.

Key words: plague, horizontal transfer, Yersinia, evolution, genomic

Running title: Chromosomal regions acquired by *Y. pestis*

To whom correspondence should be addressed.

Dr. Anne Derbise

Institut Pasteur,

Yersinia Research Unit

28, rue du Dr. Roux,

75724 Paris Cedex 15

France.

Tel: (33-1)-45-68-84-48.

Fax: (33-1)-45-68-89-54.

E-mail: anne.derbise@pasteur.fr

Abstract

Yersinia pestis, the causative agent of plague, has recently diverged from the less virulent enteropathogen *Y. pseudotuberculosis*. Its emergence has been characterized by massive genetic loss and inactivation, and limited gene acquisition. Acquired genes include two plasmids, a filamentous phage and a few chromosomal loci. The aim of this study was to characterize the chromosomal regions acquired by *Y. pestis*. Following in silico comparative analysis and PCR screening of 98 strains of *Y. pseudotuberculosis* and *Y. pestis*, we found that eight chromosomal loci (six regions: R1pe-R6pe and two coding sequences : CDS1pe-CDS2pe) specified *Y. pestis*. Signatures of integration by site specific or homologous recombination were identified for most of them. These acquisitions and the loss of ancestral DNA sequences were concentrated in a chromosomal region opposite to the origin of replication. The specific regions were acquired very early during *Y. pestis* evolution and were retained during its microevolution, suggesting that they might bring some selective advantages. Only one region (R3pe), predicted to carry a lambdoid prophage, is most likely no longer functional because of mutations. With the exception of R1pe and R2pe, which have the potential to encode a restriction/modification and a sugar transport system, respectively no functions could be predicted for the other *Y. pestis*-specific loci. To determine the role of the eight chromosomal loci in the physiology and pathogenicity of the plague bacillus, each of them was individually deleted from the bacterial chromosome. None of the deletants exhibited defects during growth in vitro. Using the *Xenopsylla cheopis* flea model, all deletants retained the capacity to produce a stable and persistent infection, and to block fleas. Similarly, none of the deletants caused any acute flea toxicity. In the mouse model of infection, all deletants were fully virulent upon subcutaneous or aerosol infections. Therefore, our results suggest that acquisition of new chromosomal materials has not been of major

54 importance in the dramatic change of life cycle that has accompanied the emergence of *Y.*
55 *pestis*.
56

Introduction

Yersinia pestis, the causative agent of plague, is a highly uniform clone that has recently diverged from the enteric pathogen *Y. pseudotuberculosis* (2). Despite their close genetic relationship, the plague bacillus and its recent ancestor differ radically in their pathogenicity and transmission. *Y. pseudotuberculosis* is transmitted by the fecal-oral route and causes enteritis of moderate intensity in Humans (48). In contrast, *Y. pestis* is transmitted by fleabites or aerosols and causes highly severe infections, i.e. bubonic and pneumonic plague (37).

The transformation of *Y. pseudotuberculosis* into *Y. pestis* has been accompanied by the acquisition of two plasmids, pFra and pPla. The 101-kb pFra plasmid is required for colonization of and survival in the flea midgut and appears to increase the efficacy of infection after flea bites (46). However, this plasmid is dispensable for *Y. pestis* pathogenicity upon subcutaneous infection in mice (18) or aerosol infection in African green monkeys (9). The 9.6-kb pPla plasmid, which encodes the plasminogen activator and protease Pla, is critical for the virulence of some *Y. pestis* strains (55). It was shown to be required for the translocation of the bacteria from their intradermal site of inoculation to the draining lymph node (49), but not for their direct dissemination to the blood stream (47). Nonetheless, recent studies have shown that *Y. pseudotuberculosis*, which is naturally deprived of pPla, can reach the lymph node draining the intradermal site of inoculation as efficiently as *Y. pestis* (19). Therefore, the stage of the infectious process during which pPla exerts its activity remains unclear. Furthermore, acquisition of pPla is not sufficient to account by itself for the dramatic rise in virulence of *Y. pestis* because there are natural isolates of *Y. pestis* that lack pPla and still are highly virulent to mice after subcutaneous injection (45, 55), and introduction of pPla in *Y. pseudotuberculosis* does not increase its virulence in mice (31, 38).

Chromosomal determinants are thus likely to be involved in the modifications in pathogenicity and life cycle that accompanied the emergence of *Y. pestis*. Surprisingly, it

appears that the transformation of the enteropathogen *Y. pseudotuberculosis* into the plague bacillus has been mostly characterized by extensive loss of genetic material and functions (8). Ten chromosomal loci conserved in the species *Y. pseudotuberculosis* have been lost by *Y. pestis* during the course of its differentiation (39, 40), and 208 genes present in the two species have been inactivated during the transformation process (8). The natural inactivation of one of these genes has recently been shown to have participated to the change in *Y. pestis* mode of transmission (51).

In contrast, only a few new chromosomal genetic materials, designated here as *Y. pestis*-specific, have been acquired during the transformation of an enteropathogen into the hyper virulent plague bacillus. One of these loci encodes a filamentous phage (YpfΦ), which is functional and participates (albeit moderately) to *Y. pestis* pathogenicity (11). Previous comparative genomic analyses of *Y. pestis* and *Y. pseudotuberculosis* have identified additional *Y. pestis*-specific genes (8, 24, 42, 56, 57). Some of these studies involved large arrays of *Y. pestis* strains (up to 260), but the number of *Y. pseudotuberculosis* isolates was always much more limited (nine or less). Similarly, while the number of *Y. pestis* genome sequences available is increasing rapidly (http://www.ncbi.nlm.nih.gov/sutils/genom_table.cgi?database=386656), only two genomes of *Y. pseudotuberculosis* have been published until now (8, 14). Nonetheless, since *Y. pseudotuberculosis* is a much older species, it displays a level of genetic polymorphism much higher than that of the relatively clonal species *Y. pestis* (2). Therefore, the delineation of *Y. pestis*-specific chromosomal regions based on the comparison with a few *Y. pseudotuberculosis* isolates could not be accurate.

In this study, a large panel of *Y. pestis* and *Y. pseudotuberculosis* strains was screened to identify chromosomal regions that specify the plague bacillus. The genetic organisation, potential mode of integration into the ancestral bacterial chromosome, putative function and

microevolutionary step at which the plague bacillus acquired these regions was studied. Finally, the role of this new genetic materials on *Y. pestis* growth, transmission and pathogenicity was evaluated.

Materials and Methods

Bacterial strains, plasmids and culture conditions. The natural *Y. pestis* and *Y. pseudotuberculosis* isolates used in this study are listed in Supplementary Tables S1 and S2. They were taken from the collection of the *Yersinia* Research Unit (Institut Pasteur). The various *Y. pestis* CO92 derivatives constructed here are described in Supplementary Table S3. All bacteria were grown in Luria-Bertani (LB), or M63S broth (KH_2PO_4, 0.1M; $(NH_4)_2SO_4$, 0.2%; $MgSO_4$, 0.02%; $FeSO_4$, 0.00005%) with 0.2% glucose and 0.2% casaminoacids, and on LB agar plates supplemented with 0.002% (w/v) hemin at 28°C or 37°C. Chloramphenicol (25 µg/ml), kanamycin (Km, 30 µg/ml), or irgasan (0.1 µg/ml) were added to the media when necessary. The pigmentation phenotype of *Y. pestis* was determined after 4 days of growth on Congo red agar plates (52). All experiments involving *Y. pestis* strains were performed in a BSL3 laboratory.

In silico analysis of *Yersinia* genomes. The genome sequences of *Y. pestis* CO92 (36) and *Y. pseudotuberculosis* IP32953 (8) were compared pairwise using the Artemis Comparison Tool (ACT) (http://www.sanger.ac.uk/Software/ACT). Re-annotation was performed using the AMIGene software (Annotation of MIcrobial Genes)(6). DNA and protein sequences were analyzed with Blast programs (3). Search for syntenies was performed with the tools implemented in the MicroScope platform (54) and available via the MaGe interface (https://www.genoscope.cns.fr/agc/mage/YersiniaScope).

DNA manipulations. Bacterial genomic DNA was extracted with the Isoquick kit (ORCA Research Inc.). All primers used for PCR amplification are listed in Supplementary Table S4. PCR were performed with 1 unit of Taq polymerase (Roche) or 1 unit of a 3:1 mixture of Taq and Pfu (Stratagene) polymerases in the supplier's buffer. PCR amplification reaction mixtures contained 10 µM of each primer and 1 mM dNTPs. The PCR program involved one step at 94°C for 5 min, followed by 35 cycles of amplification of three steps: (i) 94°C for 30s, (ii) 55°C for 30s and (iii) 72°C for 1 min. PCR products were maintained at 72°C for 7 min, electrophoresed in 1% agarose gels, and stained with ethidium bromide. DNA sequencing was performed on PCR fragments by the Millegene company.

RNA isolation and transcript analysis. RNA extraction was performed with the TRI Reagent® kit (Ambion) on 4 ml of *Y. pestis* grown to stationary phase in LB at 28°C. DNA was removed from the RNA samples by adding 4 U DNase, as described in the DNA-free kit instructions (Ambion). Total RNA was quantified by optical density at OD_{260} and 200 ng were used for reverse transcription and PCR analysis using primer pairs 623/624 (for control of RNA quality and absence of DNA) and 703A/B (for detection of YPO2469 specific mRNA transcript, Table S3).

Mutagenesis. Deletion of *Y. pestis* specific sequences was done by allelic exchange with a Km (*km*) resistance cassette, following the Short Flanking Homology procedure (12) for $R1_{pe}$ to $R5_{pe}$ and $CDS2_{pe}$, and following the Long Flanking Homology procedure (12) for $R6_{pe}$ and $CDS1_{pe}$. The Km resistance cassette was obtained by PCR amplification using plasmid pGP704N-*km* as template and primer pairs listed in Table S3. The PCR products were introduced by electroporation into *Y. pestis* CO92(pKOBEG-*sacB*), as described previously (12). Recombinant colonies were selected on Km agar plates. Correct insertion of the

157 antibiotic cassettes was verified by PCR with primers located on each side of the inserted
158 fragment (Table S3).
159
160 **Animal infections.** Prior to infection, the presence of the three plasmids was systematically
161 checked by PCR with primer pairs 157A/157B (*caf1*), 159A/159B (*pla*) and 160A/160B
162 (*yopM*). The presence of the High-Pathogenicity Island was determined by plating the *Y.*
163 *pestis* clones on Congo red agar plates. The animals used for subcutaneous (sc) and aerosol
164 infections were 5 weeks old female OF1 mice (Charles River). The animals were infected sc
165 with 10 cfu/ml of bacterial suspensions from cultures grown for 48h at 28°C on LB agar
166 plates. Aerosol infections were induced by exposing mice for 10 min to an atmosphere
167 containing droplets of a *Y. pestis* suspension (10^8 CFU/ml of saline). Droplets (1 μ m median
168 size) were generated by a Raindrop® nebulizer (Tyco, http://www.tyco.com) and were
169 introduced in an all-glass aerosol chamber deviced for a nose-only exposure of animals (34).
170 Lethality was recorded daily for 3 weeks. All animal experiments were performed in a BSL3
171 animal facility.
172
173 **Flea infections.** *Xenopsylla cheopis* fleas were infected by allowing them to feed on blood
174 containing ~5 x 10^8 CFU/ml of the various *Y. pestis* CO92 derivatives, using a previously
175 described artificial feeding system (25, 26). A sample of 20 female fleas was collected
176 immediately after the infectious blood meal, placed at -80° C, and subsequently used for CFU
177 plate count determinations of the average infectious dose per flea (25, 26, 30). An additional
178 group of 76 to 112 fleas (approximately equal numbers of males and females) that took an
179 infectious blood meal were maintained at 21 °C for four weeks, during which time they were
180 allowed to feed on uninfected mice on days 6, 9, 13, 16, 20, 23, and 27. Immediately after
181 each of these feedings all fleas were individually examined under a dissecting microscope to

182 determine how many had taken a normal blood meal (indicated by the presence of fresh red
183 blood filling the midgut) and how many were blocked (indicated by the presence of fresh red
184 blood only in the oesophagus, anterior to the proventriculus) (26). A matched group of
185 uninfected control fleas that fed on blood containing no bacteria was routinely included in
186 each infection experiment. Excess mortality (% mortality of infected fleas) – (% mortality of
187 uninfected control fleas) was recorded during the four week period after the infectious blood
188 meal. After four weeks, a final sample of 20 surviving female fleas was collected to determine
189 the infection rate and average CFU per infected flea (25, 26).
190

191 ## RESULTS AND DISCUSSION

192 **Delineation of the *Y. pestis*-specific chromosomal loci.** A previous *in silico* comparative
193 analysis of the genomes of *Y. pestis* (strains CO92 and KIM10+) and *Y. pseudotuberculosis*
194 (strain IP32953) identified 21 chromosomal clusters specific to the two *Y. pestis* genomes (8).
195 These loci were either single coding sequences (CDS) or clusters of two or more adjacent
196 genes (designated R_{pe}, for *Y. pestis*-specific regions). When the presence of these 21 clusters
197 was previously tested in a panel of 22 *Y. pestis* and *Y. pseudotuberculosis* isolates, only six
198 clusters were found to be present in all *Y. pestis* and absent from all *Y. pseudotuberculosis*
199 strains examined (8).

200 In this study we wanted to perform an in depth analysis of chromosomal regions that
201 specify *Y. pestis* in order to better understand how they might have been acquired and whether
202 they participated to the change in life cycle and pathogenicity of the plague bacillus. These
203 regions could have been acquired by *Y. pestis* after its divergence from *Y. pseudotuberculosis,*
204 but it is also possible that a few of them were horizontally acquired by the specific *Y.*
205 *pseudotuberculosis* strain from which the plague bacillus emerged, because their presence
206 was a prerequisite for *Y. pestis* emergence. Furthermore, the *Y. pestis* genome is known to

undergo rearrangements that lead to loss of genetic material, as previously shown for the High Pathogenicity Island (HPI)(10) and the filamentous phage YpfΦ (11). Taking all these considerations into account, we considered here as *Y. pestis*-specific, a locus present in most *Y. pestis* strains and absent from almost all *Y. pseudotuberculosis* isolates studied.

To identify all potentially critical regions, we proceeded in four steps: (i) the *in silico* comparative analysis of the genomes of CO92 and IP32953 was re-run, (ii) new primers were designed and used to screen the same set of 22 *Y. pestis* and *Y. pseudotuberculosis* isolates previously examined (8) to confirm the specificity of the regions studied, (iii) less stringent criteria were used to select chromosomal loci that might have participated to the emergence of the plague bacillus, and (iv) the specificity and conservation of the selected loci were then tested across a large panel of 76 additional strains of the two species. Since one of these loci corresponds to the *Y. pestis* filamentous phage YpfΦ which has already been the subject of an in depth analysis (11), this genomic region was not included in the specific regions analyzed here.

Our *in silico* genomic comparison of CO92 and IP32953 allowed us to identify, in addition to the 21 clusters previously found, two additional *Y. pestis* CDS, YPO1899 and YPO2469, that were absent from the genome of *Y. pseudotuberculosis* IP32953. These two CDS were not retained in the initial comparative analysis (8), probably because their predicted coding potential was low. However, since their functionality is unknown, we decided to keep them for further screening. The first PCR screening was then done to confirm the presence or absence of these 23 loci in the 13 *Y. pestis* belonging to the evolutionary branches 1 and 2 (1), and the 9 *Y. pseudotuberculosis* of serotypes I to V previously analyzed, with 51 pairs of primers newly designed and located within one or more ORFs of each locus (Table S1). We considered that the absence of a locus in a few *Y. pestis* strains was not sufficient to exclude it from the list of specific regions. As explained above, the transformation of *Y.*

pseudotuberculosis into *Y. pestis* was probably gradual and continuous, and consequently the presence of a locus in a single isolate of *Y. pseudotuberculosis* was not considered as a redhibitory condition for selection. Based on these criteria, 10 of the 23 initial loci were not further considered as *Y. pestis*-specific (Table S1). Despite the presence of two non-specific ORFs (YPO3946 and YPO3947) in locus 21, this region was kept for further analysis because it also contained two specific ORFs (YPO3945 and YPO3948). Altogether, 13 loci were thus retained for the second screening (Table S1). These included the five *Y. pestis*-specific clusters previously identified (8) as well as eight additional loci, of which two corresponded to the two CDS newly detected by our *in silico* comparative analysis.

The specificity of these 13 loci was further investigated using the same set of primers to screen by PCR a panel of 46 *Y. pestis* and 30 *Y. pseudotuberculosis* additional strains (Table S2). This screen showed that the genome of some *Y. pestis* strains (for instance IP539, IP537, IP540 and IP566) was prone to frequent rearrangements leading to a significant loss of genetic material. These strains were isolated during the 1950's, and their genomic rearrangements most likely occurred upon prolonged storage. It also appeared that some loci (especially YPO2469, YPO2484 and YPO3616) were frequently lost (while others were systematically conserved), suggesting both that they are located in an unstable chromosomal region and that these regions do not carry genes essential for *in vitro* survival of *Y. pestis*. Since the number of isolates was large in the second screen, we decided to retain for further physiological analyses the loci for which ≥90% of the 39 *Y. pseudotuberculosis* strains studied during the first and second screens gave a negative or weak signal. As shown in Table S2, eight loci corresponding to six regions (designated $R1_{pe}$ to $R6_{pe}$) and two CDS ($CDS1_{pe}$ and $CDS2_{pe}$) met this criterion.

After our screening was performed, the genome sequences of three other *Y. pseudotuberculosis* strains (IP31758 (14), PB1+

(http://www.ncbi.nlm.nih.gov/sites/entrez?Db=genomeprj&cmd=ShowDetailView&TermToSearch=28745), and YPIII (http://www.ncbi.nlm.nih.gov/sites/entrez?Db=genomeprj&cmd=ShowDetailView&TermToSearch=28743) became available. Blast analyses were performed between these sequenced genomes and the nucleotide sequences of the eight *Y. pestis*-specific loci selected. This genome analysis confirmed the results of the PCR screen, except for YPO3945 in $R6_{pe}$ (Table S2). Indeed, a similar sequence (97% nt identity) was found in the genomes of *Y. pseudotuberculosis* IP31758 and YPIII, although it lacked the start codon present in the *Y. pestis* sequence. A portion of YPO3945 was also found in the PB1+ genome. Sequence analysis of YPO3945 revealed that one of the primers we used to amplify this locus was located in a region exhibiting a certain degree of polymorphism, which could explain our negative PCR results. This agrees with the results of the previous study (in which other primer pairs were used), showing the presence of this sequence in several *Y. pseudotuberculosis* strains (8). Therefore, YPO3945 should not be considered as *Y. pestis*-specific. However, based on certain pecularities of $R6_{pe}$ that will be described below, we decided to keep the entire region, and not only YPO3948, for future analyses.

Organization and putative functions of the *Y. pestis*-specific chromosomal regions. The results of Blast analyses performed on the deduced amino acid sequences of each region and CDS indicated that the majority of the coding sequences are predicted to encode hypothetical proteins or proteins of unknown functions (Table S5). An in depth *in silico* analysis of the organization and putative function of each specific chromosomal locus, along with a comparison with the homologous *Y. pseudotuberculosis* regions in which each *Y. pestis*-specific locus has inserted itself, were then performed.

CDS1$_{pe}$ (YPO1899) is located at one extremity of the *Y. pestis* High Pathogenicity Island (HPI) (7), and more specifically at the 5' end of the IS*100* copy (Fig. 1A). This locus most likely corresponds to region A, previously found to be specific for the *Y. pestis* HPI (21). Its putative start codon is situated within the inverted repeat of IS*100*. The YPO1899 predicted product shares no significant similarity with proteins in data bases, but its DNA sequence contains a 159 bp region similar (70% nt identity) to the iso-IS*630* transposase of *Salmonella choleraesuis* (Genbank D10689). To determine whether YPO1899 could be a functional coding sequence, we performed a reverse transcription assay (RT-PCR) on total RNA extracted from *Y. pestis* CO92. No mRNA was detected (data not shown), arguing against its functionality. It is thus possible that this CDS is a remnant of an insertion sequence that, like IS*100*, inserted itself into a hot spot of IS integration. This is reminiscent of the local hopping of IS*3* elements found at one extremity of the *Y. enterocolitica* HPI (43).

CDS2$_{pe}$ (YPO2469) is located within a region known as Clustered Regularly Interspaced Short Palindromic Repeats (CRISPRs, Fig. 1B), which consists in 28 bp-long repeated sequences separated by 32-33 bp unique spacers (28). Addition of new spacers renders these structures highly plastic and generates a polymorphism which can be used for phylogenetic analyses (41). The fact that several *Y. pestis* strains were negative during our PCR screens (Table S2) suggests that they had lost (or not acquired) the corresponding spacers. In CO92, the CRISPR contains nine repeats whereas in IP32953 there are 18 repeats (Fig. 1B). However, the sequences in the CO92 and IP32953 spacers are different, indicating a different origin. The YPO2469 open reading frame (ORF) overlaps several 28 bp-long repeated sequences and its start and stop codons are located inside specific spacers (Fig. 1B). Because of the peculiar features of YPO2469, we also performed RT-PCR on total RNA extracted from CO92 to see whether this putative ORF is transcribed. A transcript of the expected size was indeed detected (data not shown), thus confirming that, despite its unusual location,

306 $CDS2_{pe}$ is transcribed. A putative function could not be attributed to $CDS2_{pe}$ because it has no
307 homologs in data bases. CRISPR were shown to provide resistance against phage infections
308 in prokaryotes (5), but such a function has not been demonstrated in *Y. pestis*.

309 $R1_{pe}$ is a 11.7 kb-long region which carries 11 ORFs (YPO0387-0397) in the two
310 orientations (Fig. 1C). The loci on each side of $R1_{pe}$ are not adjacent on the *Y.*
311 *pseudotuberculosis* IP32953 chromosome. It is known that despite the very close genetic
312 relationship between *Y. pestis* and *Y. pseudotuberculosis*, their chromosomes are not colinear
313 (8), most probably because of frequent rearrangements between the numerous IS present on
314 the *Y. pestis* chromosome. The presence of an IS*100* copy adjacent to $R1_{pe}$ (or in $R1_{pe}$)
315 suggests that the integration event was followed by IS-mediated chromosomal rearrangements
316 in *Y. pestis.* The very low GC content of the central ORFs in $R1_{pe}$ is suggestive of a mosaic
317 structure resulting from successive integration events. This hypothesis is reinforced by the
318 presence of remnants of transposable elements (IS*R1* and IS*21*) in this region (Table S5).
319 Most of the genes on $R1_{pe}$ are predicted to encode products with low or no homology with
320 known proteins. However, three may play a role in DNA restriction/modification. One of
321 them, located in the low GC% portion of $R1_{pe}$, would be a methylase (YPO0391), while two
322 adjacent sequences (YPO0387-0388) at the left-hand extremity of $R1_{pe}$ have the potential to
323 encode a complete restriction/modification system similar to the McrB system of *E. coli*
324 (Table S5). Remarkably, R1 appears to have been exchanged with a *Y. pseudotuberculosis*-
325 specific region (YPTB0535-0537) coding also for a restriction/modification system. This
326 region was shown to play a major role in *Y. pseudotuberculosis* pathogenicity (40).

327 $R2_{pe}$ is a 7.8 kb region composed of five CDSs (YPO1668-1672, Fig. 1D). This region has
328 inserted itself between YPTB2403 and YPTB2404 in the genome of the *Y.*
329 *pseudotuberculosis* ancestor. No mobile elements adjacent to $R2_{pe}$ could explain its
330 integration site into the *Y. pestis* genome. The YPO1672 ORF located at the right-hand

extremity of $R2_{pe}$ is predicted to encode a large protein of 1,268 aa which has two paralogs on the CO92 chromosome: YPO0765 (82% id. in 1,206 aa) and YPO0309 (81% id. in 1,199 aa). This identity concerns the last two thirds of the encoded products while their NH2 extremities are different. The conserved COOH portion of these proteins exhibits homology with a domain PL2-passenger and an autotransporter beta-domain, suggesting that they encode autotransporters proteins of a type V secretion system. Many proteins secreted by type V secretion systems have been linked to virulence in Gram-negative bacteria (22, 23). Recently, one *Y. pestis* autotransporter adhesin (YapE encoded by YPO3984) has been shown to be required for efficient colonization of the host during bubonic plague (33). The other ORFs (YPO1668 to YPO1671) carried by $R2_{pe}$ share similarity (63% to 85% id.) with CDSs of *Proteus mirabilis* that exhibit the same gene organization and that are putatively forming a sugar transport system (Table S5). Interestingly, one of the *Y. pseudotuberculosis*-specific regions ($R5_{pst}$) that was shown to have been lost during the emergence of *Y. pestis,* is also putatively involved in sugar transport (39). However, this *Y. pseudotuberculosis*-specific region was not found to be important for the physiology or pathogenicity of this species.

$R3_{pe}$ is a very large region (41.7 kb) composed of 52 ORFs (YPO2084-2136), which is predicted to be a lambda prophage (Fig. 1E and Table S5). This phage inserted itself between YPTB2404 and YPTB2405 in the genome of the *Y. pseudotuberculosis* ancestral strain, probably using its own machinery of insertion via a mechanism of site specific recombination. Indeed, an identical 31 nt repeat (ATATTGAATAAGCCGAGTTGGGCTAAATAAC) is found at each extremity of the CO92 prophage. This 31 nt sequence is found in two copies flanking the prophage in all *Y. pestis* sequenced genomes while it is present in a single copy in the *Y. pseudotuberculosis* genomes. This suggests that the 31 nt sequence served as an *att* site for phage integration and, as classically observed during chromosomal insertion of lambda phages, resulted in a

duplicated sequence upon integration. This putative prophage also carries at its left-hand extremity two genes predicted to form the phage insertion/excision machinery, i.e. an integrase (YPO2084) and an excisionase (YPO2087) (Table S5). However, the *int* gene is interrupted by the insertion of an IS*100* element which most likely inactivates it, suggesting that this phage is now stabilized in the *Y. pestis* chromosome. Another IS element (IS*285*) is found at the other extremity of the prophage and has most likely inserted itself secondarily into the phage genome. In addition to *int*, another prophage-borne gene (YPO2103) predicted to encode a terminase, which is required for cleavage of the *cos* site and therefore for the encapsidation of the phage DNA, is interrupted by an IS*285* insertion. Finally, the YPO2106 CDS (of unknown function) is truncated because of a frameshift in its nt sequence. By comparing the genetic organization of the *Y. pestis* lambdoid prophage with that of the well studied *E. coli* lambda phage, it appears that the regions coding for phage morphogenesis are similar, while the loci involved in lambda replication, regulation and recombination are absent or divergent in the *Y. pestis* phage. This along with the presence of several truncated genes and the fact that the size of the phage is drastically smaller in some *Y. pestis* strains such as Antiqua (28.6 kb), Angola (23.6 kb) or Microtus (8.9 kb), suggest that the *Y. pestis* lambda prophage is non-functional and is undergoing a process of reductive evolution. Interestingly, the lambdoid phage the closest to that of *Y. pestis* is found in the genome of *Y. enterocolitica* Ye8081 (53). Indeed, 25 of the $R3_{\mathbf{pe}}$ ORFs have homologs in a region of the Ye8081 genome predicted to be a prophage. Despite a high level of conservation of some genes, some other genes are much less conserved and some regions are different in the two prophages (Table S5), suggesting that they belong to the same phage family but that they are different or diverged long before infecting independently the *Y. enterocolitica* and *Y. pestis* branches.

380 $R4_{pe}$ is a 2.7 kb region composed of four ORFs (YPO2483-2486), all in the same
381 orientation (Fig. 1F). $R4_{pe}$ is flanked by two 98% identical 250 nt-long DNA repeats that are
382 inside the 5' portions of two coding sequences : one in YPO2486 at the left-hand extremity of
383 $R4_{pe}$, and the other one in YPO2482, bordering the right-hand extremity of $R4_{pe}$. Remarkably,
384 a segment sharing 97% and 98% nt identity with the left and right 250 nt repeats, respectively
385 is also found within the YPTB2524 coding sequence on the *Y. pseudotuberculosis*
386 chromosome (Fig. 1F). This is highly suggestive of the insertion of a circular DNA molecule
387 by homologous recombination between the 250 nt segment in YPTB2524 and the same
388 sequence carried by the incoming replicon. This integration event has probably been
389 accompanied or followed by secondary rearrangements at the site of integration since a single
390 recombination event would not be sufficient to explain the genetic organization of this region
391 in *Y. pestis.* As could be expected for an integration by a single crossing over, two fusion
392 ORFS were generated at each extremity: one composed of the entire YPTB2524 sequence
393 followed by a sequence brought by the replicon, creating YPO2486, and another mosaic ORF
394 (YPO2482) composed of a portion of YPTB2524 fused to a portion of the downstream
395 YPTB2523 CDS (Fig. 1F). Of note, another copy of the 250 nt DNA segment is found within
396 another CDSs in *Y. pestis* (YPO2490) and in *Y. pseudotuberculosis* (YPTB2527). Both these
397 CDSs have the characteristics of being located in the vicinity of the $R4_{pe}$ integration site and
398 of coding for very large proteins predicted to be hemolysins. YPO2486 also shares 38%
399 similarity with an hemolysin/hemagglutinin-like protein HecA precursor from *Erwinia*
400 *chrysanthemi* (44). The other three ORFs carried by $R4_{pe}$ (YPO2483-2485) are of unknown
401 functions. They all have a GC% lower than 39 and share little or no homology with proteins
402 in data bases, suggesting that they originate from a distantly related donor strain.

403 $R5_{pe}$ is a 3 kb-long region composed of two ORFs (YPO3436-3437). Elements involved in
404 gene mobility are found on each side: YPO3438 at the right-hand extremity encodes a

putative integrase, and at the left-hand extremity YPO3436 is truncated by the insertion of an IS*100* element, which is itself followed by an IS*1541* copy (Fig. 1G). As already observed for $R1_{pe}$, the loci on each side of $R5_{pe}$ are not adjacent on the *Y. pseudotuberculosis* IP32953 genome. Possibly, $R5_{pe}$ was part of a larger mobile element and its integration into the *Y. pestis* chromosome was associated with intra-genomic rearrangements via IS*100* recombination. Similarly to the other two CDS, the putative function of $R5_{pe}$ remains unknown because its amino acid sequence shares no significant similarity with proteins in data bases.

$R6_{pe}$ is 1.9 kb-long and is composed of four small ORFs (YPO3945-3948) in the two orientations (Fig. 1H). This region inserted itself between YPTB3789 and YPTB3790 in the ancestral *Y. pseudotuberculosis* strain. Interestingly, a perfectly conserved 15 nt-long sequence (GCGAATTCTGCTGTA) is found both between YPTB3789 and YPTB3790 on the *Y. pseudotuberculosis* IP32953 chromosome, and at the two extremities of $R6_{pe}$ on the *Y. pestis* CO92 chromosome (Fig. 1H). This is consistent with the insertion of a foreign DNA by a mechanism of site specific recombination. The analysis of the three other *Y. pseudotuberculosis* sequenced genomes indicates that all three have an element inserted at the same site, flanked by the 15 nt repeat (Fig. S1). This argues for the 15 nt sequence being a hot spot of integration of foreign DNA. This 15 nt repeat is identical to that of *Y. pestis* on one side, and is slightly divergent (caGtAATCTGCTGTA) on the other side. The imported DNA has a common backbone (represented by strain YPIII), in which different DNA sequences have inserted themselves, either before or after integration at the 15 nt site. Remarkably, in *Y. pseudotuberculosis* IP31758, the incoming DNA has created a large ORF, either by fusion with the two bordering sequences, or more likely by allelic replacement between these sequences and a larger ORF having the same extremities. Also remarkable is the observation that in *Y. pestis* YPO3945, a potential start codon is located just upstream of the 15 nt repeat

of *Y. pestis,* while in *Y. pseudotuberculosis*, the slight divergence in the repeat introduces a stop codon which leads to a shorter ORF. Therefore, despite the conservation of the region overlapping YPO3945 in *Y. pestis* and several *Y. pseudotuberculosis* strains, the coding capacity and function of this DNA sequence might be different. No function could be predicted for the four ORFs carried by $R6_{pe}$ based on Blast analyses. From the above data, we can thus hypothesize that $R6_{pe}$ corresponds to a mobile element which can insert itself into bacterial chromosomes by site specific recombination, and which carries a conserved core sequence and a variable region in which different CDSs are found inserted. Whether the *Y. pestis* region was horizontally acquired after its divergence from *Y. pseudotuberculosis* or whether it was vertically acquired from an ancestor that had an identical region cannot be determined. However, the fact that none of the screened *Y. pseudotuberculosis* strains harbored YPO3948 and that the 15 nt right-hand repeat is different between the two species argues for the first hypothesis.

Altogether, it thus appears that, based on the scars left by the insertion of the eight *Y. pestis*-specific chromosomal loci, a mechanism of acquisition can be predicted for most of them. The position of these loci on the *Y. pestis* CO92 chromosome indicates that six out of nine (when the YpfΦ genome is considered) are located in the region opposite to the origin of replication (Fig. 2). Similarly, most of the regions lost by *Y. pestis* (i.e. *Y. pseudotuberculosis*-specific) are also located in this part of the chromosome (Fig. 2). The genetic polymorphism in bacterial chromosomes is known to be the highest in this portion of the chromosome, which contains the *dif* site where resolution of chromosomal dimers takes place during bacterial division (50). Indeed, more than one third of the acquisition or loss of genetic materials (from $R4_{pe}$ to $R2_{pst}$, Fig. 2) in *Y. pestis* are concentrated in a region which represents only 5% of the entire *Y. pestis* chromosome. In two instances, the acquisition of the *Y. pestis*-specific loci seems to have occurred by exchange with a *Y. pseudotuberculosis*-specific region

455 ($R3_{pst}$ replaced by YpfΦ, and $R6_{pst}$ by $R1_{pe}$). In terms of functions, with the exception of $R1_{pe}$,
456 $R2_{pe}$, and $R3_{pe}$, which putatively encode a restriction/modification system, a sugar transporter
457 and a lambdoid phage, respectively, no specific function could be attributed to the other five
458 loci. It is noteworthy that no putative virulence factor was identified on any of the eight *Y.*
459 *pestis*-specific chromosomal loci studied.
460
461 **History of the acquisition and modification of the specific regions during *Y. pestis***
462 **microevolution.** We wondered whether the eight specific regions studied here were acquired
463 early or late after *Y. pestis* emergence from *Y. pseudotuberculosis*. A previous molecular
464 phylogenetic study allowed us to design a microevolution tree for *Y. pestis* and to delineate a
465 set of Single Nucleotide Polymorphisms (SNPs) that could be used to position a new isolate
466 on this tree (1). Today, the complete genome sequences of 21 *Y. pestis* strains (Microtus
467 91001, pestoides A, pestoides F, Angola, Antiqua B42003004, Nepal 516, KIM10,
468 K1973002, Antiqua, UG05-0454, E1979001, D106004, D182038, IP275, CA88-4125,
469 F1991016, MG05-1020, FV-1, India 195, PEXU 2 and CO92) are available (listed in
470 http://www.ncbi.nlm.nih.gov/sutils/genom_table.cgi?database=386656), but their position
471 along the microevolutionary tree is not known for most of them. To draw an updated tree, a
472 subset of 16 SNPs defining the main branches and sub-branches were selected among those
473 previously identified (1), and their presence/absence was checked in the 21 genomes. This
474 allowed us to position all strains for which no branching was yet assigned in the *Y. pestis*
475 updated microevolution tree (Fig. 3). The position of *Y. pestis* pestoides A was confirmed
476 using a second set of SNPs along the 0.PE4 branch. Furthermore, based on the presence or
477 absence of the s1 SNP, the 1.ANT strains could be differentiated into two sub-branches (the
478 $1.ANT_1$ and $1.ANT_2$, Fig. 3). The presence of the eight *Y. pestis*-specific loci was then
479 examined in these 21 *Y. pestis* genomes.

480 CDS2$_{pe}$ is a peculiar case because it is located within a CRISPR, which has the
481 characteristics of being highly plastic and of generating a polymorphism (41). We could
482 nonetheless observe in our PCR screens that this CDS is present in only a portion of Antiqua
483 and Medievalis strains, while it is found in all 23 Orientalis strains analyzed (Table S2). All
484 seven other specific loci were present in the genomes of all 21 sequenced *Y. pestis* isolates,
485 including Pestoides strains which were not available for our PCR screens (Fig. 3). This
486 indicates that these seven loci were acquired very early during *Y. pestis* evolution, before the
487 split of the most ancient branch (0.PE4) along branch 0. It also indicates that these regions
488 were stably kept during the microevolution of the plague bacillus.

489 In a previous analysis of *Y. pestis* housekeeping genes, we were unable to identify a single
490 polymorphic nt at 21,881 synonymous sites within 36 *Y. pestis* strains because this species is
491 remarkably monomorphic (2). We wondered whether this was also the case for the seven
492 horizontally acquired regions, or whether peculiar mutations could specify some evolutionary
493 branches. A detailed analysis of these regions at the gene level indicated a very high degree of
494 nt conservation, with nonetheless some polymorphisms. CDS1$_{pe}$ was completely
495 monomorphic in the 21 genomes analyzed and R5$_{pe}$ was also identical in 20 genomes except
496 in Angola, which is known to be a very atypical strain (15). Among various reasons that could
497 explain this absence of polymorphism, one could be that these two regions were subjected to
498 a strong selective pressure because they encode functions important for *Y. pestis* life cycle.
499 However, another and more likely explanation is that, because of their small size, the chances
500 of acquiring point mutations or deletions/insertions are lower.

501 For the other regions, a few sequence variations were observed, and some of these
502 variations were informative in terms of *Y. pestis* microevolution. Indeed several
503 SNPs/deletion in R1$_{pe}$ and R3$_{pe}$ were characteristic of branch 0 and of the 0.PE4, and 0.PE2
504 branches that split off along this branch early during evolution (Fig. 3 and Table S6). SNPb in

505 $R1_{pe}$ occurred before the separation between branches 1 and 2 and thus characterizes all
506 classical *Y. pestis* strains of branches 1 and 2. Along branch 2, one SNP in $R3_{pe}$ defines the
507 2.MED sub-branch. On branch 1, one SNP in $R2_{pe}$ (Table S6) specified the 11 strains (three
508 $1.ANT_2$ and eight 1.ORI) the most recently emerged along this branch 1 and confirmed the
509 1.ANT split evidenced by the s1 SNP (Fig. 3). Curiously, the older $1.ANT_1$ sub-branch was
510 characterized by mutations, including inactivating deletions (Table S6), in three specific
511 regions ($R1_{pe}$, $R3_{pe}$ and $R6_{pe}$, Fig. 3).

512 Overall, $R1_{pe}$ and $R3_{pe}$ were the two specific regions in which the highest rates of genetic
513 polymorphisms were observed. The fact that these regions are the two largest in size could
514 explain at least in part their higher polymorphism. $R3_{pe}$ corresponds to the lambdoid prophage
515 genome. The fact that deletions of large regions predicted to encode phage functions required
516 to infect a bacterial host occurred in different branches (YPO2095 to YPO2135 in branch
517 0.PE4, and YPO2087 to YPO2103 in $1.ANT_1$ sub-branch, Fig. 3) suggests a single
518 acquisition event and further argues for a secondary process of reductive evolution. This,
519 along with our above observation that some genes necessary for the phage physiology are
520 inactivated in all strains support the hypothesis that a functional phage is not necessary for *Y.*
521 *pestis* life cycle and/or virulence. The polymorphism of $R1_{pe}$ was the highest but
522 corresponded mostly to SNPs that occurred in different genes without inactivating them
523 (Table S6). Even the small 6 nt deletion that arose early along branch 0 (but which could also
524 be a 6 nt insertion in branch 0.PE4) was in frame and therefore did not disrupt the coding
525 sequence. Except for the presence of a putative DNA restriction/modification system, most of
526 the genes carried by $R1_{pe}$ have no predicted functions. The absence of inactivating mutations
527 in this region, whatever the genes involved and the evolutionary branch, supports the
528 hypothesis that this region may be useful for *Y. pestis* physiological or pathological processes.
529

Mutagenesis of the *Y. pestis* acquired regions and impact on bacterial physiological and pathogenic properties. To investigate the role of the eight specific chromosomal loci on the ability of *Y. pestis* to grow *in vitro*, to infect fleas and to kill mice, each locus was individually deleted by allelic exchange with a kanamycin cassette. The ORFs encompassed by the deletions and the primers used to check that the replacements occurred as expected are indicated on Fig. 1 and in Table S4. The resulting deletion strains with their designation are listed in Table S3. To perform the deletions using the lambda red technology, the pKOBEG-*sacB* plasmid was introduced into *Y. pestis* strain CO92, yielding CO92p (Table S3). Since the chromosome of *Y. pestis* is prone to frequent rearrangements (20), and since we found that the presence of pKOBEG-*sacB* had no significant impact on *Y. pestis* pathogenicity, we decided not to remove this plasmid in the deletion mutants, in order to limit as much as possible subcultures which would increase the occurrence of genomic reassortments. During our previous analysis of *Y. pseudotuberculosis*-specific regions, we found that two CDSs (YPTB1495 and YPTB3368) were not deletable because they are essential for IP32953 survival (40). This was not the case for the *Y. pestis*-specific loci as the eight specific regions were successfully deleted.

To determine whether some of these loci play a role in the ability of *Y. pestis* to multiply *in vitro*, the CO92p parental strain and the eight deletants were cultured in LB at 28°C (optimal temperature for *Yersinia* growth) and 37°C (*in vivo* temperature). No growth defects were observed in the various mutants as compared to the CO92p parental strain (data not shown). Similar results were previously obtained with the various *Y. pseudotuberculosis* strains deleted of each specific region (40). However, when these *Y. pseudotuberculosis* deletants were grown in the biochemically defined medium M63S, a growth defect could be observed for several mutants. The ability of the eight *Y. pestis* deletants and the parental CO92p strain to grow in the M63S medium at 28°C and 37°C was thus tested and compared. The growth

curves of all strains were comparable, both at 28°C and 37°C (data not shown). Therefore, none of the eight *Y. pestis*-acquired chromosomal loci are required for optimal bacterial growth, at least under the experimental conditions used here.

A major difference during the transformation of *Y. pseudotuberculosis* into *Y. pestis* has been a switch in the mode of transmission, from the oral route to flea bites. It could thus be expected that some of the chromosomal regions that specify *Y. pestis* participated to its adaptation to its new transmission cycle. This has been demonstrated for the two *Y. pestis*-specific plasmids: pFra is necessary for an efficient colonization of and survival in the flea midgut (27), as well as for an efficient transmission by fleas (46), whereas pPla is important for the dissemination of the bacteria from the intradermal inoculation site to the draining lymph node (47, 49). A key feature of *Y. pestis* that facilitates flea-borne transmission, and that differentiates it from *Y. pseudotuberculosis,* is its capacity to block fleas. This blockage is due to the formation of a biofilm produced by the products of the chromosomal *hms* genes (29). Although *Y. pseudotuberculosis* harbors similar *hms* genes, this species does not block fleas (16), indicating that other genetic determinants participate to this activity. To determine whether the acquired regions could play a role in the capacity of *Y. pestis* to infect and block fleas, groups of 76 to 112 *X. cheopis* were artificially fed on blood containing similar inocula ($1.5x10^8$ to $1x10^9$ CFU/ml) of each of the eight deletants or CO92p, and monitored for blockage during a four week period after infection. As shown in Fig. 4A, blockage developed in all of the flea groups at a rate expected for the *X. cheopis*-*Y. pestis* infection model (26, 27), indicating that none of the *Y. pestis*-specific loci is required for biofilm development in the flea proventriculus. Because fleas that become blocked can no longer take a blood meal, they rapidly starve to death. Thus, excess mortality can be used as an indirect indicator of blockage. In keeping with their ability to block fleas, all groups of infected fleas had elevated excess mortality rates of 15-58%, which is typical for *X. cheopis* fleas infected with *Y. pestis*

580 (27). The eight mutants also were able to produce a stable, persistent infection in the flea at
581 rates equivalent to that of CO92p (Fig. 4B). The average bacterial load in infected fleas after 4
582 weeks was high for all the *Y. pestis* strains tested, ranging from $1.2x10^4$ to $7.9x10^5$ CFU/flea.
583 In *X. cheopis*, it has been shown that *Y. pestis* has gained the capacity to colonize the flea
584 gut without causing major damages during the early phase of infection, whereas its *Y.*
585 *pseudotuberculosis* progenitor exerts acute toxic effects on these insects (17). None of the
586 eight deletants or CO92p caused any acute toxicity to the fleas that took an infectious blood
587 meal, indicating that none of the *Y. pestis*-specific chromosomal loci play an essential role in
588 the lower toxicity of *Y. pestis* for fleas.
589 One of the major differences between *Y. pestis* and its ancestor *Y. pseudotuberculosis* is the
590 acquisition by the former of an exceptional pathogenicity potential. Although the horizontally
591 acquired pPla plasmid plays a major role in the virulence of most *Y. pestis* isolates, the fact
592 that it is dispensable in some strains (32, 45, 55) and that its introduction into *Y.*
593 *pseudotuberculosis* is not accompanied by an increase in virulence (31, 38) clearly indicates
594 that other factors are required. One of them has been shown to be the YpfΦ filamentous phage
595 (11), but other *Y. pestis*-acquired chromosomal loci may have also played a role in this gain of
596 virulence. However, using the mouse model of subcutaneous infection to mimic bubonic
597 plague, the eight mutants were found to be as virulent as the parental strain CO92p (Table 1).
598 *Y. pestis* has also acquired the capacity to be transmitted by aerosols and to cause pneumonic
599 plague. The capacity of the eight mutants to produce a lethal infection upon aerosol
600 inoculation was tested by exposing mice to aerosolized droplets of a suspension containing
601 10^8 CFU/ml (three times the LD_{50}). All deletants killed 100% of the infected animals with a
602 mean time to death similar to that of the CO92p strain (Table 1), Altogether, these results
603 suggest that the acquired regions and CDSs studied here did not participate in the increased

pathogenicity of *Y. pestis,* at least in our experimental mouse models of sc and aerosol infections.

Conclusions. Our study has identified eight chromosomal loci that were acquired soon before or early after the divergence of *Y. pestis* from *Y. pseudotuberculosis*. Surprisingly, we were unable to evidence an impact of these regions under *in vitro* and *in vivo* conditions. It is possible that acquisition of these regions provided no benefit to the bacterial host and, because *Y. pestis* is a recently emerged bacterium, that they did not have yet the time to be inactivated and eliminated by gradual mutations and/or deletions. This could be the case for the lambdoid phage ($R3_{pe}$) in which several genes predicted to encode physiological functions are interrupted, as well as for $CDS1_{pe}$ which is probably a remnant of an insertion element and which is no longer transcribed. This is also true for many other genes in *Y. pestis* whose genome is characterized by a massive gene inactivation (8). However, the fact that the other regions, which were acquired early during *Y. pestis* microevolution, are conserved and potentially functional in the various evolutionary sub-branches, suggests that they have been subjected to a positive selective pressure for their maintenance, and thereby that they should confer advantages at some steps of the *Y. pestis* biological cycle. If so, our inability to attribute a physiological role to these loci may have several reasons. One possible explanation would be that the functions of two or more acquired regions are redundant. Multiple deletions of the *Y. pestis*-acquired loci would thus be needed to observe a defect. In the flea model, although no effect on toxicity or proventriculus blockage was observed, it is still possible that the deletion of some loci had an impact on the efficiency of flea transmission, as recently observed for the F1 capsule (46). Furthermore, since *Y. pestis* can be transmitted by many different flea species, some of which do not develop proventricular blockage to the same extent as *X. cheopis* (13), testing the various mutants in other flea models might also be of

interest. The absence of virulence impairment in the various deletants indicates that none of the *Y. pestis*-specific regions play a major role in *Y. pestis* pathogenicity. However, because of the extreme pathogenicity of the plague bacillus in the mouse model, minor virulence defects might be difficult to evidence. The use of more resistant animal models could potentially unable the identification of subtle virulence impediments. Finally, *Y. pestis* has been shown to be able to survive in naturally contaminated soils for several weeks (4) and in burrows of wild rodents for several years (35). The assumption that the acquired regions could participate to the long-term persistence of the plague bacillus outside an insect vector or a mammalian host may also be considered. Whatever the reasons for the absence of identified roles, our results suggest that, unlike what might have been assumed, acquisition of new chromosomal materials has not been of major importance in the dramatic change of life cycle that has accompanied the emergence of *Y. pestis.*

Acknowledgements

This study was funded in part by contract DGA 99 01110004709450 from the French Defense Ministry and a fellowship for A. D. from the Pasteur-Weissman foundation.

References

1. **Achtman, M., G. Morelli, P. Zhu, T. Wirth, I. Diehl, B. Kusecek, A. J. Vogler, D. M. Wagner, C. J. Allender, W. R. Easterday, V. Chenal-Francisque, P. Worsham, N. R. Thomson, J. Parkhill, L. E. Lindler, E. Carniel, and P. Keim.** 2004. Microevolution and history of the plague bacillus, *Yersinia pestis*. Proc Natl Acad Sci U S A **101:**17837-17842.

2. **Achtman, M., K. Zurth, G. Morelli, G. Torrea, A. Guiyoule, and E. Carniel.** 1999. *Yersinia pestis*, the cause of plague, is a recently emerged clone of *Yersinia pseudotuberculosis*. Proc Natl Acad Sci U S A **96:**14043-14048.

3. **Altschul, S. F., T. L. Madden, A. A. Schaffer, J. Zhang, Z. Zhang, W. Miller, and D. J. Lipman.** 1997. Gapped BLAST and PSI-BLAST: a new generation of protein database search programs. Nucleic Acids Res **25:**3389-3402.

4. **Ayyadurai, S., L. Houhamdi, H. Lepidi, C. Nappez, D. Raoult, and M. Drancourt.** 2008. Long-term persistence of virulent *Yersinia pestis* in soil. Microbiology **154:**2865-2871.

5. **Barrangou, R., C. Fremaux, H. Deveau, M. Richards, P. Boyaval, S. Moineau, D. A. Romero, and P. Horvath.** 2007. CRISPR provides acquired resistance against viruses in prokaryotes. Science **315:**1709-1712.

6. **Bocs, S., S. Cruveiller, D. Vallenet, G. Nuel, and C. Medigue.** 2003. AMIGene: Annotation of MIcrobial Genes. Nucleic Acids Res **31:**3723-3726.

7. **Buchrieser, C., M. Prentice, and E. Carniel.** 1998. The 102-kilobase unstable region of *Yersinia pestis* comprises a high-pathogenicity island linked to a pigmentation segment which undergoes internal rearrangement. J Bacteriol **180:**2321-2329.

8. **Chain, P. S., E. Carniel, F. W. Larimer, J. Lamerdin, P. O. Stoutland, W. M. Regala, A. M. Georgescu, L. M. Vergez, M. L. Land, V. L. Motin, R. R. Brubaker, J. Fowler, J. Hinnebusch, M. Marceau, C. Medigue, M. Simonet, V. Chenal-Francisque, B. Souza, D. Dacheux, J. M. Elliott, A. Derbise, L. J. Hauser, and E. Garcia.** 2004. Insights into the evolution of *Yersinia pestis* through whole-genome comparison with *Yersinia pseudotuberculosis*. Proc Natl Acad Sci U S A **101:**13826-13831.

9. **Davis, K. J., D. L. Fritz, M. L. Pitt, S. L. Welkos, P. L. Worsham, and A. M. Friedlander.** 1996. Pathology of experimental pneumonic plague produced by fraction 1-positive and fraction 1-negative *Yersinia pestis* in African green monkeys *Cercopithecus aethiops*. Arch Pathol Lab Med **120:**156-163.

10. **de Almeida, A. M., A. Guiyoule, I. Guilvout, I. Iteman, G. Baranton, and E. Carniel.** 1993. Chromosomal *irp2* gene in Yersinia: distribution, expression, deletion and impact on virulence. Microb Pathog **14:**9-21.

11. **Derbise, A., V. Chenal-Francisque, F. Pouillot, C. Fayolle, M. C. Prevost, C. Medigue, B. J. Hinnebusch, and E. Carniel.** 2007. A horizontally acquired filamentous phage contributes to the pathogenicity of the plague bacillus. Mol Microbiol **63:**1145-1157.

12. **Derbise, A., B. Lesic, D. Dacheux, J. M. Ghigo, and E. Carniel.** 2003. A rapid and simple method for inactivating chromosomal genes in Yersinia. FEMS Immunol Med Microbiol **38:**113-116.

13. **Eisen, R. J., S. W. Bearden, A. P. Wilder, J. A. Montenieri, M. F. Antolin, and K. L. Gage.** 2006. Early-phase transmission of *Yersinia pestis* by unblocked fleas as a mechanism explaining rapidly spreading plague epizootics. Proc Natl Acad Sci U S A **103:**15380-15385.

14. **Eppinger, M., M. J. Rosovitz, W. F. Fricke, D. A. Rasko, G. Kokorina, C. Fayolle, L. E. Lindler, E. Carniel, and J. Ravel.** 2007. The complete genome sequence of *Yersinia pseudotuberculosis* IP31758, the causative agent of Far East scarlet-like fever. PLoS Genet **3:**e142.

15. **Eppinger, M., P. L. Worsham, M. P. Nikolich, D. R. Riley, Y. Sebastian, S. Mou, M. Achtman, L. E. Lindler, and J. Ravel.** Genome sequence of the deep-rooted

Yersinia pestis strain Angola reveals new insights into the evolution and pangenome of the plague bacterium. J Bacteriol.

16. **Erickson, D. L., C. O. Jarrett, B. W. Wren, and B. J. Hinnebusch.** 2006. Serotype differences and lack of biofilm formation characterize *Yersinia pseudotuberculosis* infection of the Xenopsylla cheopis flea vector of *Yersinia pestis*. J Bacteriol **188:**1113-1119.

17. **Erickson, D. L., N. R. Waterfield, V. Vadyvaloo, D. Long, E. R. Fischer, R. Ffrench-Constant, and B. J. Hinnebusch.** 2007. Acute oral toxicity of *Yersinia pseudotuberculosis* to fleas: implications for the evolution of vector-borne transmission of plague. Cell Microbiol **9:**2658-2666.

18. **Friedlander, A. M., S. L. Welkos, P. L. Worsham, G. P. Andrews, D. G. Heath, G. W. Anderson, Jr., M. L. Pitt, J. Estep, and K. Davis.** 1995. Relationship between virulence and immunity as revealed in recent studies of the F1 capsule of *Yersinia pestis*. Clin Infect Dis **21 Suppl 2:**S178-181.

19. **Guinet, F., P. Ave, L. Jones, M. Huerre, and E. Carniel.** 2008. Defective innate cell response and lymph node infiltration specify *Yersinia pestis* infection. PLoS One **3:**e1688.

20. **Guiyoule, A., B. Rasoamanana, C. Buchrieser, P. Michel, S. Chanteau, and E. Carniel.** 1997. Recent emergence of new variants of *Yersinia pestis* in Madagascar. J Clin Microbiol **35:**2826-2833.

21. **Hare, J. M., A. K. Wagner, and K. A. McDonough.** 1999. Independent acquisition and insertion into different chromosomal locations of the same pathogenicity island in *Yersinia pestis* and *Yersinia pseudotuberculosis*. Mol Microbiol **31:**291-303.

22. **Henderson, I. R., and J. P. Nataro.** 2001. Virulence functions of autotransporter proteins. Infect Immun **69:**1231-1243.

725 23. **Henderson, I. R., F. Navarro-Garcia, M. Desvaux, R. C. Fernandez, and D.**
726 **Ala'Aldeen.** 2004. Type V protein secretion pathway: the autotransporter story.
727 Microbiol Mol Biol Rev **68:**692-744.
728 24. **Hinchliffe, S. J., K. E. Isherwood, R. A. Stabler, M. B. Prentice, A. Rakin, R. A.**
729 **Nichols, P. C. Oyston, J. Hinds, R. W. Titball, and B. W. Wren.** 2003. Application
730 of DNA microarrays to study the evolutionary genomics of *Yersinia pestis* and
731 *Yersinia pseudotuberculosis*. Genome Res **13:**2018-2029.
732 25. **Hinnebusch, B. J., K. L. Gage, and T. G. Schwan.** 1998. Estimation of vector
733 infectivity rates for plague by means of a standard curve-based competitive
734 polymerase chain reaction method to quantify *Yersinia pestis* in fleas. Am J Trop Med
735 Hyg **58:**562-569.
736 26. **Hinnebusch, B. J., R. D. Perry, and T. G. Schwan.** 1996. Role of the *Yersinia pestis*
737 hemin storage (hms) locus in the transmission of plague by fleas. Science **273:**367-
738 370.
739 27. **Hinnebusch, B. J., A. E. Rudolph, P. Cherepanov, J. E. Dixon, T. G. Schwan, and**
740 **A. Forsberg.** 2002. Role of Yersinia murine toxin in survival of *Yersinia pestis* in the
741 midgut of the flea vector. Science **296:**733-735.
742 28. **Jansen, R., J. D. van Embden, W. Gaastra, and L. M. Schouls.** 2002. Identification
743 of a novel family of sequence repeats among prokaryotes. OMICS **6:**23-33.
744 29. **Jarrett, C. O., E. Deak, K. E. Isherwood, P. C. Oyston, E. R. Fischer, A. R.**
745 **Whitney, S. D. Kobayashi, F. R. DeLeo, and B. J. Hinnebusch.** 2004. Transmission
746 of *Yersinia pestis* from an infectious biofilm in the flea vector. J Infect Dis **190:**783-
747 792.

30. **Jarrett, C. O., F. Sebbane, J. J. Adamovicz, G. P. Andrews, and B. J. Hinnebusch.** 2004. Flea-borne transmission model to evaluate vaccine efficacy against naturally acquired bubonic plague. Infect Immun **72:**2052-2056.

31. **Kutyrev, V., R. J. Mehigh, V. L. Motin, M. S. Pokrovskaya, G. B. Smirnov, and R. R. Brubaker.** 1999. Expression of the plague plasminogen activator in *Yersinia pseudotuberculosis* and *Escherichia coli*. Infect Immun **67:**1359-1367.

32. **Kutyrev, V. V., A. A. Filippov, N. Shavina, and O. A. Protsenko.** 1989. Genetic analysis and simulation of the virulence of *Yersinia pestis*. Mol Gen Mikrobiol Virusol**:**42-47.

33. **Lawrenz, M. B., J. D. Lenz, and V. L. Miller.** 2009. A novel autotransporter adhesin is required for efficient colonization during bubonic plague. Infect Immun **77:**317-326.

34. **Leif, W. R., and A. P. Krueger.** 1950. Studies on the experimental epidemiology of respiratory infections. I. An apparatus for the quantitative study of air-borne respiratory pathogens. J Infect Dis **87:**103-116.

35. **Mollaret, H. H.** 1968. Conservation du bacille de la peste durant 28 mois en terrier artificiel : démonstration expérimentale de la conservation interépizootique de la peste dans ses foyers invétérés. Comptes rendus de l'Académie des Sciences de Paris **267:**972-973.

36. **Parkhill, J., B. W. Wren, N. R. Thomson, R. W. Titball, M. T. Holden, M. B. Prentice, M. Sebaihia, K. D. James, C. Churcher, K. L. Mungall, S. Baker, D. Basham, S. D. Bentley, K. Brooks, A. M. Cerdeno-Tarraga, T. Chillingworth, A. Cronin, R. M. Davies, P. Davis, G. Dougan, T. Feltwell, N. Hamlin, S. Holroyd, K. Jagels, A. V. Karlyshev, S. Leather, S. Moule, P. C. Oyston, M. Quail, K. Rutherford, M. Simmonds, J. Skelton, K. Stevens, S. Whitehead, and B. G.**

Barrell. 2001. Genome sequence of *Yersinia pestis*, the causative agent of plague. Nature **413:**523-527.

37. **Perry, R. D., and J. D. Fetherston.** 1997. *Yersinia pestis*--etiologic agent of plague. Clin Microbiol Rev **10:**35-66.

38. **Pouillot, F., A. Derbise, M. Kukkonen, J. Foulon, T. K. Korhonen, and E. Carniel.** 2005. Evaluation of O-antigen inactivation on Pla activity and virulence of *Yersinia pseudotuberculosis* harbouring the pPla plasmid. Microbiology **151:**3759-3768.

39. **Pouillot, F., C. Fayolle, and E. Carniel.** 2007. A putative DNA adenine methyltransferase is involved in *Yersinia pseudotuberculosis* pathogenicity. Microbiology **153:**2426-2434.

40. **Pouillot, F., C. Fayolle, and E. Carniel.** 2008. Characterization of chromosomal regions conserved in *Yersinia pseudotuberculosis* and lost by *Yersinia pestis*. Infect Immun **76:**4592-4599.

41. **Pourcel, C., G. Salvignol, and G. Vergnaud.** 2005. CRISPR elements in *Yersinia pestis* acquire new repeats by preferential uptake of bacteriophage DNA, and provide additional tools for evolutionary studies. Microbiology **151:**653-663.

42. **Radnedge, L., P. G. Agron, P. L. Worsham, and G. L. Andersen.** 2002. Genome plasticity in *Yersinia pestis*. Microbiology **148:**1687-1698.

43. **Rakin, A., S. Schubert, I. Guilvout, E. Carniel, and J. Heesemann.** 2000. Local hopping of IS*3* elements into the A+T-rich part of the high-pathogenicity island in *Yersinia enterocolitica* 1B, O:8. FEMS Microbiol Lett **182:**225-229.

44. **Rojas, C. M., J. H. Ham, W. L. Deng, J. J. Doyle, and A. Collmer.** 2002. HecA, a member of a class of adhesins produced by diverse pathogenic bacteria, contributes to the attachment, aggregation, epidermal cell killing, and virulence phenotypes of

Erwinia chrysanthemi EC16 on *Nicotiana clevelandii* seedlings. Proc Natl Acad Sci U S A **99:**13142-13147.

45. **Samoilova, S. V., L. V. Samoilova, I. N. Yezhov, I. G. Drozdov, and A. P. Anisimov.** 1996. Virulence of pPst+ and pPst- strains of *Yersinia pestis* for guinea-pigs. J Med Microbiol **45:**440-444.

46. **Sebbane, F., C. Jarrett, D. Gardner, D. Long, and B. J. Hinnebusch.** 2009. The *Yersinia pestis* caf1M1A1 fimbrial capsule operon promotes transmission by flea bite in a mouse model of bubonic plague. Infect Immun **77:**1222-1229.

47. **Sebbane, F., C. O. Jarrett, D. Gardner, D. Long, and B. J. Hinnebusch.** 2006. Role of the *Yersinia pestis* plasminogen activator in the incidence of distinct septicemic and bubonic forms of flea-borne plague. Proc Natl Acad Sci U S A **103:**5526-5530.

48. **Smego, R. A., J. Frean, and H. J. Koornhof.** 1999. Yersiniosis I: microbiological and clinicoepidemiological aspects of plague and non-plague Yersinia infections. Eur J Clin Microbiol Infect Dis **18:**1-15.

49. **Sodeinde, O. A., Y. V. Subrahmanyam, K. Stark, T. Quan, Y. Bao, and J. D. Goguen.** 1992. A surface protease and the invasive character of plague. Science **258:**1004-1007.

50. **Steiner, W. W., and P. L. Kuempel.** 1998. Sister chromatid exchange frequencies in *Escherichia coli* analyzed by recombination at the dif resolvase site. J Bacteriol **180:**6269-6275.

51. **Sun, Y. C., B. J. Hinnebusch, and C. Darby.** 2008. Experimental evidence for negative selection in the evolution of a *Yersinia pestis* pseudogene. Proc Natl Acad Sci U S A **105:**8097-8101.

822 52. **Surgalla, M. J., and E. D. Beesley.** 1969. Congo red-agar plating medium for
823 detecting pigmentation in *Pasteurella pestis*. Appl Microbiol **18:**834-837.
824 53. **Thomson, N. R., S. Howard, B. W. Wren, M. T. Holden, L. Crossman, G. L.**
825 **Challis, C. Churcher, K. Mungall, K. Brooks, T. Chillingworth, T. Feltwell, Z.**
826 **Abdellah, H. Hauser, K. Jagels, M. Maddison, S. Moule, M. Sanders, S.**
827 **Whitehead, M. A. Quail, G. Dougan, J. Parkhill, and M. B. Prentice.** 2006. The
828 complete genome sequence and comparative genome analysis of the high
829 pathogenicity *Yersinia enterocolitica* strain 8081. PLoS Genet **2:**e206.
830 54. **Vallenet, D., S. Engelen, D. Mornico, S. Cruveiller, L. Fleury, A. Lajus, Z. Rouy,**
831 **D. Roche, G. Salvignol, C. Scarpelli, and C. Medigue.** 2009. MicroScope: a
832 platform for microbial genome annotation and comparative genomics. Database
833 (Oxford) **2009:**bap021.
834 55. **Welkos, S. L., A. M. Friedlander, and K. J. Davis.** 1997. Studies on the role of
835 plasminogen activator in systemic infection by virulent *Yersinia pestis* strain C092.
836 Microb Pathog **23:**211-223.
837 56. **Zhou, D., Y. Han, E. Dai, D. Pei, Y. Song, J. Zhai, Z. Du, J. Wang, Z. Guo, and R.**
838 **Yang.** 2004. Identification of signature genes for rapid and specific characterization of
839 *Yersinia pestis*. Microbiol Immunol **48:**263-269.
840 57. **Zhou, D., Y. Han, Y. Song, Z. Tong, J. Wang, Z. Guo, D. Pei, X. Pang, J. Zhai, M.**
841 **Li, B. Cui, Z. Qi, L. Jin, R. Dai, Z. Du, J. Bao, X. Zhang, J. Yu, P. Huang, and R.**
842 **Yang.** 2004. DNA microarray analysis of genome dynamics in *Yersinia pestis*:
843 insights into bacterial genome microevolution and niche adaptation. J Bacteriol
844 **186:**5138-5146.
845
846

847 **Legends**

848 **Figure 1. Genetic organization of the eight chromosomal loci acquired by *Y. pestis* and**
849 **comparison with the homologous regions in *Y. pseudotuberculosis*.**

850 White arrows indicate CDSs present in *Y. pestis* CO92 but not in *Y. pseudotuberculosis*
851 IP32953. Dark grey arrrows are CDSs harboring >98% nt identity betwen *Y. pestis* and *Y.*
852 *pseudotuberculosis*. Light grey areas represent the conserved regions on each side of the
853 acquired loci. Dashed lines with arrows below each region indicate the DNA fragments that
854 have been replaced by a kanamycin cassette, and the numbers at each extremity correspond to
855 the primer pairs used to generate the fragment to be deleted. In panel B, grey rectangles
856 corresponds to repeats identical in *Y. pseudotuberculosis* and *Y. pestis*. In panel F, the 250 nt-
857 long DNA repeats found at the borders of $R4_{pe}$ are indicated by black rectangles. In panel E
858 and H, black circles represent direct repeated sequences found at the extremities of each
859 region, and their size in nt are indicated below. In panel H, dashed arrows indicate ORFs that
860 are conserved in *Y. pestis* and *Y. pseudotuberculosis* although they might have been acquired
861 independently (see Fig. S1 for a more detailed comparison of this region).

862

863 **Figure 2. Position of the regions acquired and lost by *Y. pestis* on a schematic map of the**
864 **CO92 chromosome.**

865 The position on the *Y. pestis* CO92 chromosome of all loci acquired or lost by *Y. pestis* are
866 shown by black and grey arrows, respectively. The putative mechanisms of acquisition are
867 indicated next to each *Y. pestis*-specific regions.

868

869 **Figure 3**. ***Y. pestis*** **microevolution tree with the steps at which the specific regions are**
870 **predicted to have been acquired or to have undergone various mutations**.

871 The 21 *Y. pestis* strains for which a complete genome sequence was available were positioned
872 on the microevolutionary tree based on the presence or absence of a set of 16 SNPs (inside
873 white ovals) shown to characterize the various *Y. pestis* phylogenetic branches (1). To
874 position strain Pestoides A, additional SNPs defining branch 0.PE4 were examined. Among
875 them, some were present (sA: s95, s96, s97, s99, s102, s104, s105, s114, s116 and s120),
876 while others were absent (sB: s94, s98, s100, s101, s106, s107, s108, s109, s110, s111, s112,
877 s113, s115, s117, s118 and s119). The hatched rectangle corresponds to the position in the
878 tree where the *Y. pestis*-specific regions are predicted to have been acquired. The various
879 mutations in specific regions that characterize phylognentic branches are indicated by an
880 arrow and a grey rectangle which contains the type of mutation (SNP or partial deletion, ΔP)
881 and the locus involved. A more detailed description of these mutations is presented in Table
882 S6.
883
884 **Figure 4. Infection and blockage rates in fleas that fed on blood containing wild type or**
885 **mutant *Y. pestis* strains.** (A) Percentage of fleas that developed proventricular blockage
886 during a four-week period following the infectious blood meal. (B) Percentage of fleas
887 infected four weeks after the infectious blood meal. Vertical lines indicate the range of four
888 independent experiments with the wild-type strain.
889

Table 1: Virulence for mice of the *Y. pestis* recombinant strains after subcutaneous (sc) injection or aerosols exposure.

	sc		Aerosols		
Strains	CFU injected	#dead/total animal infected	suspension nebulized CFU/ml	#dead/total animal infected	mean time to death
CO92p	12	3/5	$0.95 \pm 0.3 \times 10^{8}$ [a]	12/12[a]	4 ± 1 days[a]
CO92⊗R1$_{pe}$	10	3/5	1.1×10^{8}	6/6	4.5 days
CO92⊗R2$_{pe}$	16	3/5	2×10^{8}	6/6	3 days
CO92⊗R3$_{pe}$	12	3/5	1.5×10^{8}	6/6	3 days
CO92 ⊗R4$_{pe}$	12	3/5	1.4×10^{8}	5/5	4 days
CO92 ⊗R5$_{pe}$	9	3/5	1.4×10^{8}	6/6	3 days
CO92 ⊗R6$_{pe}$	17	5/5	1.1×10^{8}	6/6	3 days
CO92 ⊗CDS1$_{pe}$	14	5/5	0.9×10^{8}	6/6	4 days
CO92 ⊗CDS2$_{pe}$	13	3/5	0.6×10^{8}	6/6	3 days

[a] Values are means ± standard deviations of two experiments with six mice each.

Fig. 1

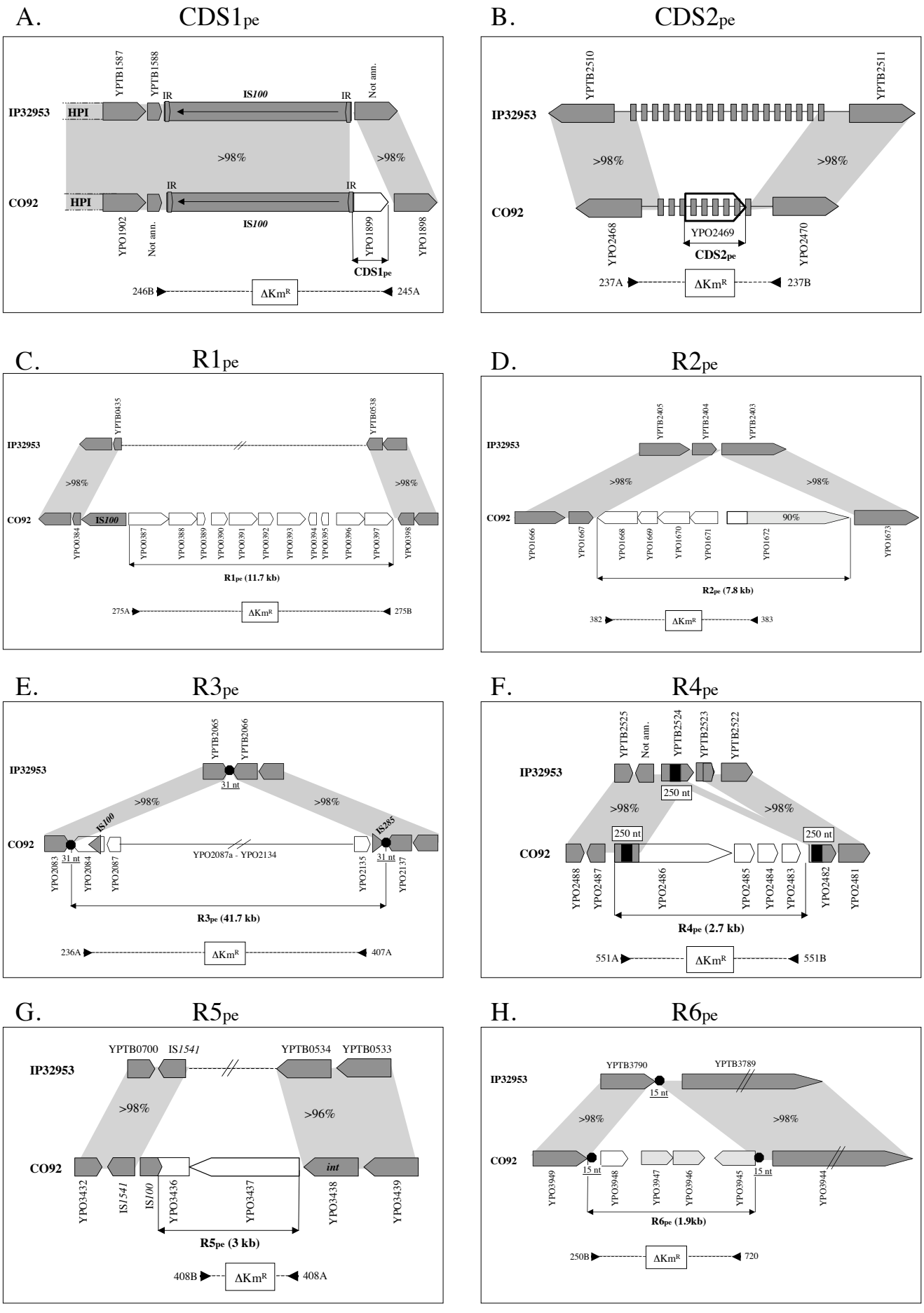
A.
CDS1pe
YPTB1587
YPTB1588
IR
IS100
IR
Not ann.
IP32953
HPI
>98%
>98%
CO92
HPI
IR
IR
IS100
YPO1902
Not ann.
YPO1899
YPO1898
CDS1pe
246B
ΔKmR
245A
B.
CDS2pe
YPTB2510
YPTB2511
IP32953
>98%
>98%
CO92
YPO2468
YPO2469
YPO2470
CDS2pe
237A
ΔKmR
237B
C.
R1pe
YPTB0435
YPTB0538
IP32953
>98%
>98%
CO92
IS100
YPO0384
YPO0387
YPO0388
YPO0389
YPO0390
YPO0391
YPO0392
YPO0393
YPO0394
YPO0395
YPO0396
YPO0397
YPO0398
R1pe (11.7 kb)
275A
ΔKmR
275B
D.
R2pe
YPTB2405
YPTB2404
YPTB2403
IP32953
>98%
>98%
CO92
90%
YPO1666
YPO1667
YPO1668
YPO1669
YPO1670
YPO1671
YPO1672
YPO1673
R2pe (7.8 kb)
382
ΔKmR
383
E.
R3pe
YPTB2065
YPTB2066
IP32953
31 nt
>98%
>98%
IS100
IS285
CO92
31 nt
YPO2087a - YPO2134
31 nt
YPO2083
YPO2084
YPO2087
YPO2135
YPO2137
R3pe (41.7 kb)
236A
ΔKmR
407A
F.
R4pe
YPTB2525
Not ann.
YPTB2524
YPTB2523
YPTB2522
IP32953
250 nt
>98%
>98%
250 nt
250 nt
CO92
YPO2488
YPO2487
YPO2486
YPO2485
YPO2484
YPO2483
YPO2482
YPO2481
R4pe (2.7 kb)
551A
ΔKmR
551B
G.
R5pe
YPTB0700
IS1541
YPTB0534
YPTB0533
IP32953
>98%
>96%
CO92
int
YPO3432
IS1541
IS100
YPO3436
YPO3437
YPO3438
YPO3439
R5pe (3 kb)
408B
ΔKmR
408A
H.
R6pe
YPTB3790
YPTB3789
IP32953
15 nt
>98%
>98%
CO92
15 nt
15 nt
YPO3949
YPO3948
YPO3947
YPO3946
YPO3945
YPO3944
R6pe (1.9kb)
250B
ΔKmR
720

Fig. 2

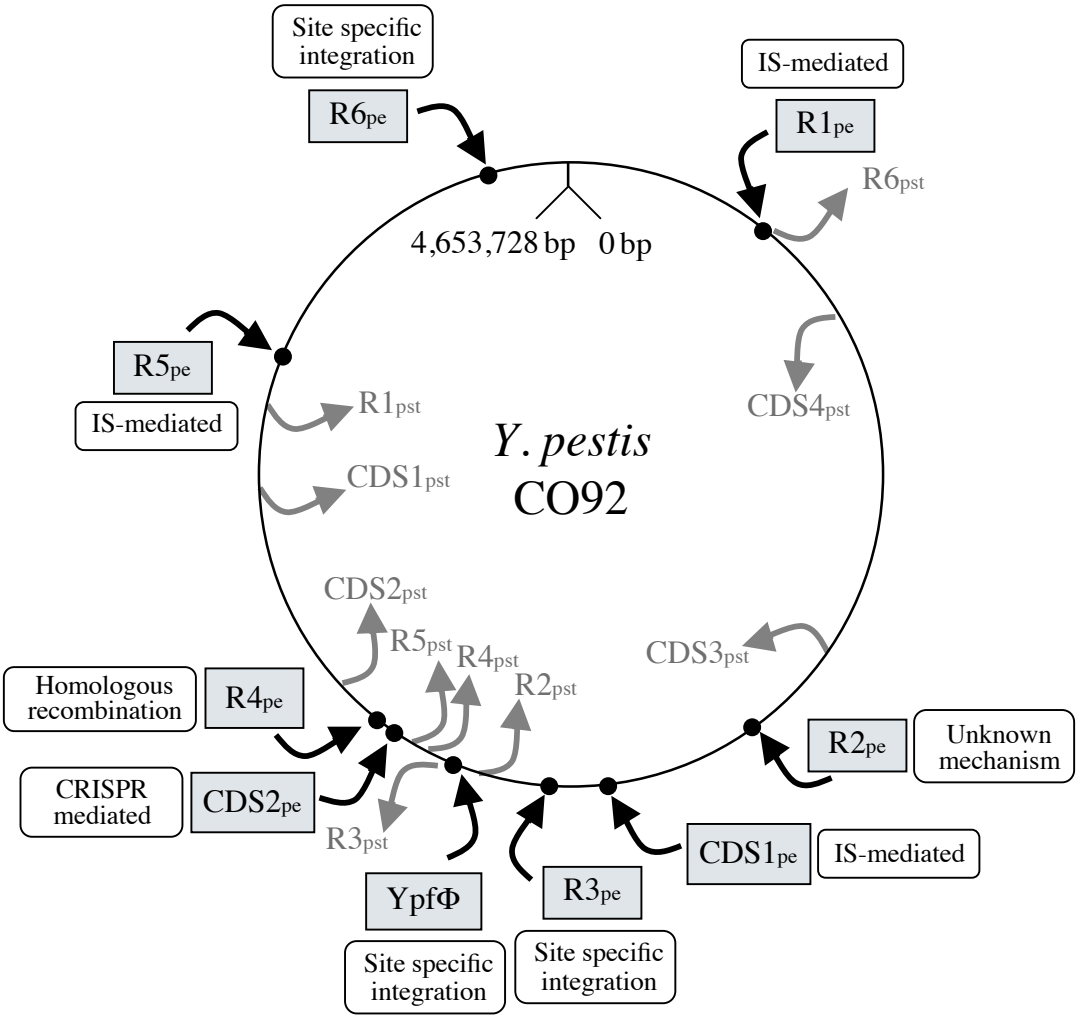
Site specific integration
R6pe
IS-mediated
R1pe
R6pst
4,653,728 bp
0 bp
R5pe
IS-mediated
R1pst
CDS1pst
Y. pestis
CO92
CDS4pst
CDS2pst
R5pst
R4pst
R2pst
CDS3pst
Homologous recombination
R4pe
CRISPR mediated
CDS2pe
R3pst
R2pe
Unknown mechanism
CDS1pe
IS-mediated
YpfΦ
Site specific integration
R3pe
Site specific integration

Fig. 3

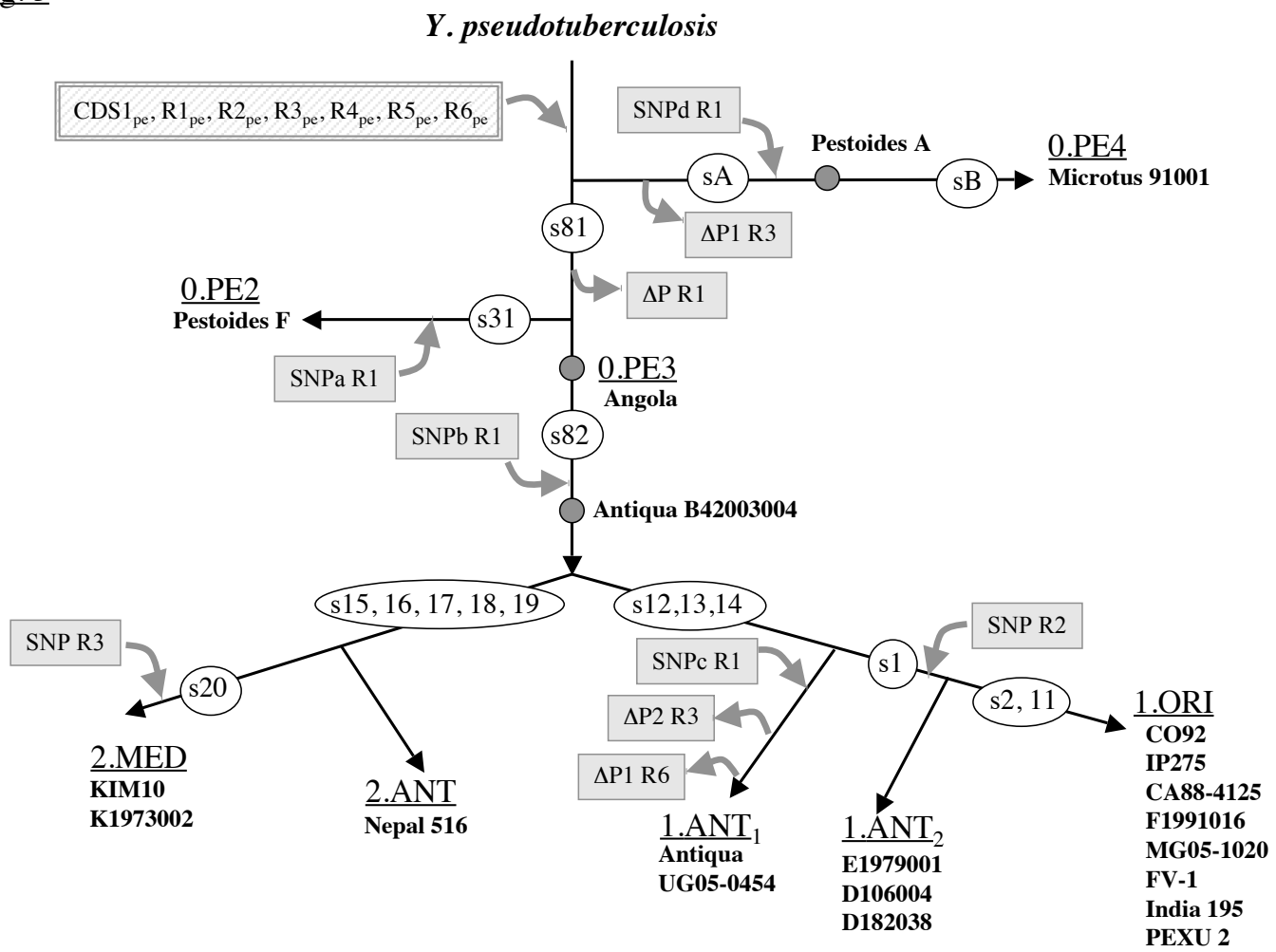
Y. pseudotuberculosis
CDS1pe, R1pe, R2pe, R3pe, R4pe, R5pe, R6pe
SNPd R1
Pestoides A
0.PE4
Microtus 91001
sA
sB
ΔP1 R3
s81
ΔP R1
0.PE2
Pestoides F
s31
SNPa R1
0.PE3
Angola
SNPb R1
s82
Antiqua B42003004
s15, 16, 17, 18, 19
s12,13,14
SNP R3
SNP R2
SNPc R1
s20
s1
ΔP2 R3
s2, 11
1.ORI
CO92
IP275
CA88-4125
F1991016
MG05-1020
FV-1
India 195
PEXU 2
ΔP1 R6
2.MED
KIM10
K1973002
2.ANT
Nepal 516
1.ANT1
Antiqua
UG05-0454
1.ANT2
E1979001
D106004
D182038

Fig. 4

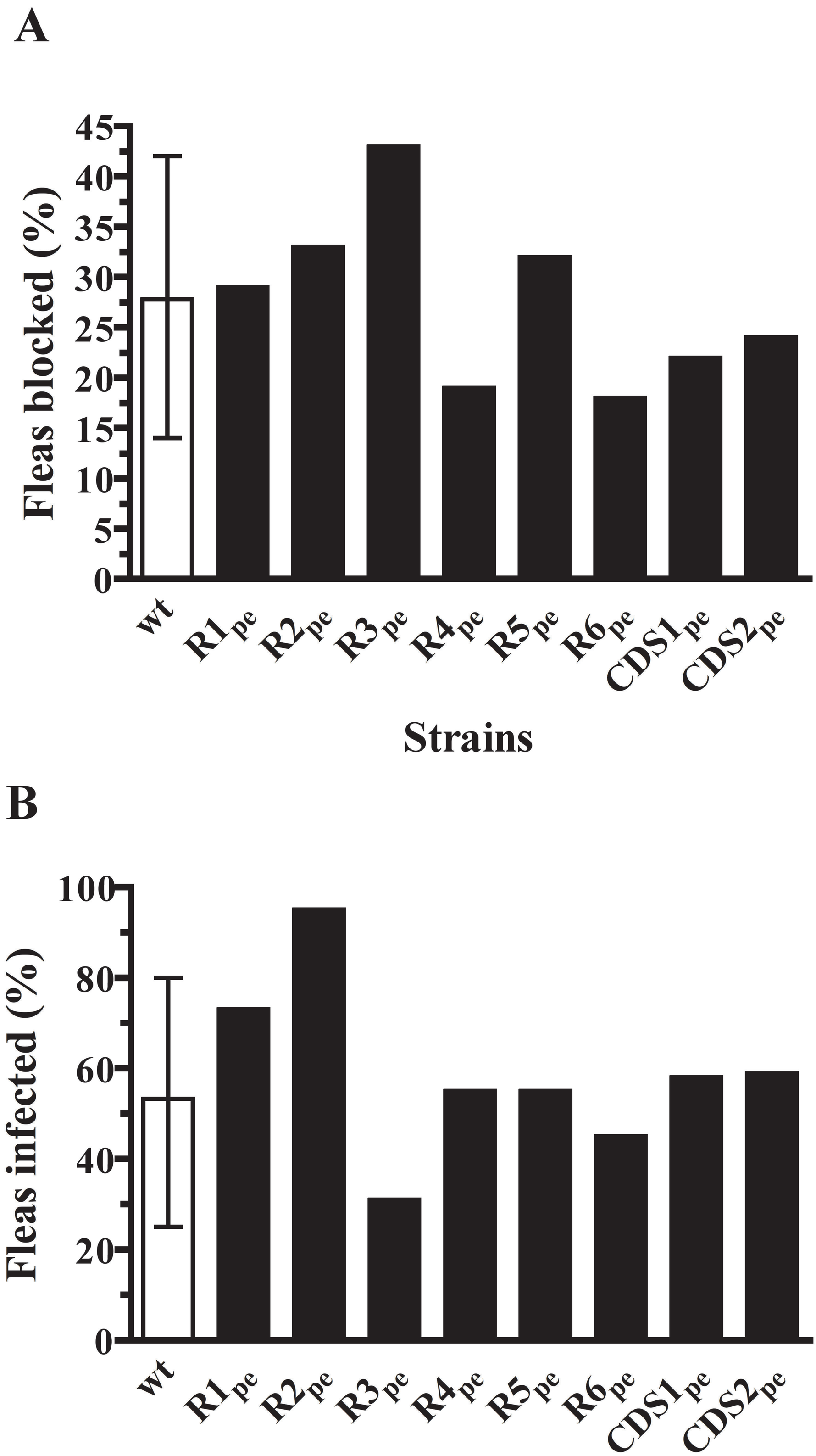
A
Fleas blocked (%)
0
5
10
15
20
25
30
35
40
45
wt
R1pe
R2pe
R3pe
R4pe
R5pe
R6pe
CDS1pe
CDS2pe
Strains
B
Fleas infected (%)
0
20
40
60
80
100
wt
R1pe
R2pe
R3pe
R4pe
R5pe
R6pe
CDS1pe
CDS2pe
Strains